A TRAIL-TL1A Paracrine Network Involving Adipocytes, Macrophages, and Lymphocytes Induces Adipose Tissue Dysfunction Downstream of E2F1 in Human Obesity

Nitzan Maixner,[1,2,3] Tal Pecht,[1,2] Yulia Haim,[1,2] Vered Chalifa-Caspi,[2] Nir Goldstein,[1] Tania Tarnovscki,[1] Idit F. Liberty,[3,4] Boris Kirshtein,[3,4] Rachel Golan,[5] Omer Berner,[6] Alon Monsonego,[6] Nava Bashan,[1,3] Matthias Blüher,[7] and Assaf Rudich[1,2,3]

Diabetes 2020;69:2310–2323 | https://doi.org/10.2337/db19-1231

Elevated expression of E2F1 in adipocyte fraction of human visceral adipose tissue (hVAT) associates with a poor cardiometabolic profile. We hypothesized that beyond directly activating autophagy and MAP3K5 (ASK)–MAP kinase signaling, E2F1 governs a distinct transcriptome that contributes to adipose tissue and metabolic dysfunction in obesity. We performed RNA sequencing of hVAT samples from age-, sex-, and BMI-matched patients, all obese, whose visceral E2F1 protein expression was either high (E2F1^{high}) or low (E2F1^{low}). Tumor necrosis factor superfamily (TNFSF) members, including *TRAIL* (*TNFSF10*), *TL1A* (*TNFSF15*), and their receptors, were enriched in E2F1^{high}. While *TRAIL* was equally expressed in adipocytes and stromal vascular fraction (SVF), *TL1A* was mainly expressed in SVF, and TRAIL-induced *TL1A* was attributed to CD4$^+$ and CD8$^+$ subclasses of hVAT T cells. In human adipocytes, TL1A enhanced basal and impaired insulin-inhibitable lipolysis and altered adipokine secretion, and in human macrophages it induced foam cell biogenesis and M1 polarization. Two independent human cohorts confirmed associations between TL1A and TRAIL expression in hVAT and higher leptin and IL6 serum concentrations, diabetes status, and hVAT-macrophage lipid content. Jointly, we propose an intra-adipose tissue E2F1-associated TNFSF paracrine loop engaging lymphocytes, macrophages, and adipocytes, ultimately contributing to adipose tissue dysfunction in obesity.

Obesity, defined as abnormal or excessive fat accumulation that presents a risk to health, was recognized as a disease by the American Medical Association in 2013 (1). However, with its increasing global prevalence, obesity is highly heterogeneous in the degree of health risks it imposes and presents itself differently even in patients with similarly elevated BMI. With the increasing quest for personalized health care, there is an urgent need to better subtype obesity (2). Compared to persons with cardiometabolically benign obesity (arguably termed "healthy/insulin-sensitive/metabolically normal obesity"), in persons with "high–cardiometabolic risk obesity" adipose tissues differ in distribution, morphology, cellular composition, molecular patterns, and function (3). Initial findings indicate that such differences, particularly morphological (adipocyte size, fibrosis) may be of assistance in subphenotyping of obesity, not only in cross-sectional analyses, but also in prediction of the clinical response to obesity interventions (4). Yet, molecular fingerprinting of adipose tissue that could serve to better stratify, prioritize, or even personalize clinical care is largely still lacking.

We identified a transcriptional molecular network in visceral adipose tissue (VAT) of patients with metabolically dysfunctional obesity (5,6). A central "hub" in this network is the transcription factor E2F1, which, when upregulated,

[1]Department of Clinical Biochemistry and Pharmacology, Faculty of Health Science, Ben-Gurion University of the Negev, Beer-Sheva, Israel
[2]The National Institute of Biotechnology in the Negev, Ben-Gurion University of the Negev, Beer-Sheva, Israel
[3]The Joyce & Irving Goldman Medical School, Ben-Gurion University of the Negev, Beer-Sheva, Israel
[4]Soroka Academic Medical Center, Beer-Sheva, Israel
[5]Department of Epidemiology and Preventive Medicine, Faculty of Health Science, Ben-Gurion University of the Negev, Beer-Sheva, Israel
[6]Department of Microbiology and Immunology, Faculty of Health Science, Ben-Gurion University of the Negev, Beer-Sheva, Israel
[7]Department of Medicine, University of Leipzig, Leipzig, Germany

Corresponding authors: Nitzan Maixner, nitzanm7@gmail.com, and Assaf Rudich, rudich@bgu.ac.il

Received 17 December 2019 and accepted 24 July 2020

This article contains supplementary material online at https://doi.org/10.2337/figshare.12709595.

N.M. and T.P. contributed equally to this work.

drives aberrant expression and activation of a MAP kinase signaling cascade (ASK1-MKK4-p38 MAPK/JNK), and of autophagy (5,6). E2F1, like other E2F family members, is a major regulator of cell-cycle progression. In adipose tissue, however, E2F1's functions are not well characterized. In obesity, elevated adipose tissue E2F1 expression originates mainly from the adipocytes (6), while during adipogenesis E2F1 acts as an adipogenic stimulator (7) and negatively regulates energy expenditure and mitochondrial activity (8). In myocytes, E2F1 favors glycolysis over glucose oxidation by activating pyruvate dehydrogenase kinase 4 (PDK4) (9). In pancreatic β-cells, it upregulates the expression of *Kir6.2* and thus glucose-stimulated insulin secretion (10). Yet, E2F1-knockout mice are not diabetic due to increased insulin sensitivity (11), suggesting a role for E2F1 in decreasing insulin responsiveness. In the liver, E2F1 overexpression supports lipid accumulation and steatosis, evidently tied to obesity and insulin resistance (12), and also drives hyperglycemia by facilitating gluconeogenesis (13). E2F1 is also highly activated in multiple inflammatory states (14), acting upstream and/or downstream of inflammatory signals, offering a putative link between obesity, low-grade inflammation, and cardiometabolic complications.

Consistent with this notion, we found that VAT E2F1 protein and mRNA levels correlated with multiple clinical indicators of high cardiometabolic risk, an effect mediated by direct E2F1 binding to promoter regions of ASK1 and autophagy genes (5,6). Yet, multivariate analyses that adjusted for the activation of these putative effector genes of E2F1 suggested that additional pathways mediate the link between increased VAT E2F1 and metabolic dysfunction (5,6). In this study, we used unbiased transcriptomic analysis of $E2F1^{high}$ versus $E2F1^{low}$ human VAT (hVAT) to delineate such possible pathways. We followed $E2F1^{high}$-associated tumor necrosis factor superfamily (TNFSF) members that this analysis revealed, and we uncovered a putative intricate intercellular paracrine network within adipose tissue, involving adipocytes, macrophages, and T cells, linking high VAT E2F1 expression with adipose tissue dysfunction.

RESEARCH DESIGN AND METHODS

Human Cohorts and VAT Samples

Participants were from the Beer-Sheva, Israel ($n = 123$), and Leipzig, Germany ($n = 421$), cohorts (Table 1) with use of coordinated procedures as previously described (5). Briefly, following approval by the ethics committees of the two centers and obtaining of written informed consent, participants (18–75 years old) were recruited before undergoing elective abdominal surgeries (bariatric or other elective procedures). After overnight fasting, blood samples were drawn and analyzed by the clinical biochemistry and endocrinology laboratories. Visceral (omental) adipose tissue biopsies were obtained during surgery and immediately delivered to the laboratory, where they were processed for mRNA or protein expression using coordinated procedures, as previously described (5). For obtaining human adipose tissue explants, tissue samples were carefully cut and cultured in MEM-Alpha containing 4.5 mmol/L glucose, 10% FBS, 2 mmol/L L-glutamine, and 100 units/mL penicillin-streptomycin for 24 h recovery. Human TRAIL (hTRAIL) (375-TEC-010; D&R Systems) 25 or 100 ng/mL was added to fresh serum-free media for 24 h treatment. Adipocyte and stromal vascular (SVF) fractions were prepared by collagenase (C6885-5G; Sigma-Aldrich) digestion as previously described (15).

Table 1—Clinical characteristics of participants from the Leipzig and Beer-Sheva cohorts

	Study cohort	
	Leipzig cohort	Beer-Sheva cohort
n	421	123
Age (years)	46.2 ± 11	40.2 ± 13
Sex (% female)	72	64
BMI (kg/m^2)	49.8 ± 9	40.25 ± 9.2
Fasting glucose (mg/dL)	124.3 ± 54	109.7 ± 36
TG (mg/dL)	178.3 ± 80	151.4 ± 46
LDL (mg/dL)	120.3 ± 32.8	116.7 ± 29
HDL (mg/dL)	45.6 ± 19.3	41.7 ± 8.5

Values are means ± SD.

Cell Cultures

Human monocyte-derived macrophages (MDM) and T cells were isolated, following approval by the Soroka Academic Medical Center Institutional Review Committee, from peripheral blood samples (100 mL) of healthy volunteers, who signed a written informed consent. Peripheral blood mononuclear cells (PBMC) were obtained from PBS–2% FBS–EDTA (2 mmol/L)–diluted plasma mounted on Ficol Lymphocytes Separation Medium (50494; MP Biomedicals), incubated for 20 min with CD14 microbeads, and transferred through magnetic columns (130-050-201 and 130-042-401, respectively; Miltenyi Biotech) to isolate monocytes. To obtain MDM, we cultured monocytes in growth media (RPMI-1640, 10% FBS, 2% L-glutamine, and 1% antibiotics) containing M-CSF 50 ng/mL (300-25; PeproTech), GM-CSF 50 ng/mL (300-03; PeproTech), or M-CSF + IL4 20 ng/mL for M0/M1/M2 polarization, respectively. Following a 6-day culture period, functional assays were conducted as further described below. The nonmonocyte ($CD14^-$) cell fraction was cultured on anti-human CD3 antibody (Ab) (300314; BioLegend)–coated plates to isolate T cells, with similar growth media. Chub-S7 cells were cultured in DMEM containing 4.5 mmol/L glucose, 20% FBS, 2 mmol/L L-glutamine, and 100 units/mL penicillin-streptomycin, until 24 h postconfluence. Differentiation was induced by addition of 1 mmol/L dexamethasone, 0.5 mmol/L 3-isobutyl-1-methylxanthine (IBMX), 10 mg/mL insulin, and 10 mmol/L rosiglitazone to the medium for 14–21 days, until the appearance of adipocyte morphology, at which stage cells exhibited robust upregulation of adipocyte genes (Supplementary Fig. 1). When differentiated, cells were cultured with

either control serum-free media or serum-free media containing human recombinant (hr)TL1A (1319-TL-010; D&R Systems) or hrTRAIL for 24 h. TL1A and TRAIL concentration range used was based on previous cell-culture studies in the literature (16,17). For insulin stimulation, Chubs-S7 were serum starved for 24 h, PBS washed, and stimulated with insulin at 37°C for 7 min.

Tissue and Cell Lysates and Western Blot Analysis

Preparation of tissue/cell lysates and antibodies used has previously been described (6). For E2F1 protein determination, we used anti-E2F1 monoclonal Ab by GeneTex (GTX-70154; GeneTex, Irvine, CA).

RNA Extraction, Quantitative Real-time PCR, and RNA-Sequencing Analysis

RNA extraction, cDNA generation, and RT-PCR amplification were conducted as previously detailed (6). RNA sequencing (RNA-seq) was performed at the Technion Genome Centre (Israel Institute of Technology, Haifa, Israel) using Illumina technology. Bioinformatics analysis was performed using the NeatSeq-Flow platform (18) and R. Raw sequences were quality trimmed and filtered using Trim Galore!, and alignment of the reads to the human genome (assembly GRCh38.p10) was done with STAR (19). Number of reads per gene per sample was counted using RSEM (20). Raw read counts were loaded into R and analyzed with DESeq2 (21). For quality assessment diagnostic plots, counts were log2 transformed, normalized, and subjected to variance-stabilizing transformation. Principal component analysis showed that sample number 5 was an outlier, highly separable from all other samples. Therefore, this sample along with its matched pair number 6 was excluded from further analyses. The design formula for paired statistical testing included the matched pair number in addition to the E2F1 condition ("~Matched_pair+E2F1"). For each gene, *P* value, false discovery rate (FDR)-adjusted *P* value, and fold change were computed for the E2F1 effect. Fold change values were expressed in linear scale. To expand the search for TNF/TNFSF genes associated with E2F1 level, we carried out an enrichment test versus a manually assembled data set of 54 TNFSF genes using Gene Set Enrichment Analysis (GSEA) standalone software. Analysis was done using DESeq2-normalized counts of all genes considering absolute change values between high to low E2F1.

Other Assays

Leptin and adiponectin levels in conditioned media of Chub-S7 and in human serum were measured as previously (6). Lactate dehydrogenase (LDH) release from Chub-S7 adipocytes was measured using the Lactate Dehydrogenase Activity Assay Kit (MAK066-1KT; Sigma-Aldrich). Released LDH was calculated as percentage of total (medium / medium + cells). hTRAIL secretion to conditioned media was measured using Immunoquantitative TRAIL ELISA (RayBio). Lipolysis was measured as previously described (22), with adenosine deaminase (ADA) at 1 μU/mL and insulin's antilipolytic effect after 24 h insulin starvation.

Macrophage Lipid Accumulation

MDM were differentiated as described in 96-well μClear, black, plates (Greiner-Bio One). M0 MDM were treated with control or TL1A 25 ng/mL serum-free media for 24 h. Lipid accumulation in fatty acid–enriched conditions was done by adding 10 mmol/L oleic acid for the final 2-h incubation as previously described (23). Cells were fixed with 4% formaldehyde followed by staining with BODIPY 493/503 (1 μg/mL) (D3922; Thermo Fisher Scientific, Waltham, MA) and DAPI (5 ng/mL) (62248; Thermo Fisher Scientific) for 20 min at room temperature and then washed with Ca^{+2}/Mg^{+2}-supplemented PBS (02-020-1A; Biological Industries). Images were acquired in a fully automated, unbiased manner using a ×40 wide angle lens–equipped microscope (Operetta; PerkinElmer, Waltham, MA). Statistical analysis was done using Columbus software (PerkinElmer).

Flow Cytometry of VAT SVF

After 3 h stimulation with or without hTRAIL, SVF cells were washed with FACS buffer and stained for membranal antigens (BioLegend, San Diego, CA) anti–CD3-FITC, CD4-BV510, CD8-AF700, and viability dye 780. Then, after 20 min paraformaldehyde fixation, cell were permeabilized and stained with anti–TL1A-PerCP-cy5.5 following the instructions of eBioscience's FoxP3 intracellular staining kit. Samples were analyzed by a Beckman Coulter CytoFLEX flow cytometer and FlowJo software.

Coculture Assays

Differentiated M0 MDM, generated as described, were cultured on permeable inserts with 0.4-μm high-density pores (353494; Falcon) and treated with control versus TL1A 25 ng/mL serum-free media for 24 h. After thorough PBS washing, inserts were transferred into Chub-S7–containing plates and cocultured in serum-free Chub-S7 growth media. After 24 h, conditioned media was collected and leptin/adiponectin levels were measured as previously described (6).

Statistical Analysis

For in vitro/ex vivo experiments, calculations were made using GraphPad. Statistically significant differences between groups were evaluated using unpaired Student *t* test/Mann-Whitney. Correlations were assessed by either Pearson or Spearman rank-order correlation tests as indicated. For human cohort data, statistical analysis was done using SPSS Statistics (version 20). Correlations were assessed using Pearson correlation test. Statistically significant differences in clinical parameters between groups were evaluated using unpaired Student *t* test.

Data and Resource Availability

The data sets generated in the current study are available from the corresponding authors upon request.

RESULTS

VAT of Patients With Obesity and High E2F1 Expression Displays a Unique Transcriptome

To identify differentially regulated pathways associated with the dysmetabolic phenotype of obese $E2F1^{high}$ VAT,

we used RNA-seq. To assess the range of VAT E2F1 expression, we measured E2F1 protein levels in VAT samples (as in previously described [6]) from $n = 67$ patients undergoing elective abdominal surgeries. VAT E2F1 levels were divided into quintiles, and the two lower and higher quintiles (the lowest and highest 40%) were defined as E2F1^{low} and E2F1^{high}, respectively (middle E2F1 expression quintile was excluded to minimize misclassification bias) (Fig. 1*A*). We matched pairs of patients with BMI $\geq$30 kg/m^2 from the E2F1^{low} and E2F1^{high} subgroups for age, sex, and BMI (Fig. 1*B–D*). Patients with VAT E2F1^{low} and E2F1^{high} ($n = 8$ in each group, with a 3:5 male:female ratio) (subcohort 1 [Table 2]) were, respectively, 41.25 and 40.25 years old (average), had an average BMI of 40.5 and 41.5 kg/m^2, and were comparable in terms of blood pressure and diabetes status.

Matched statistical analyses of the RNA-seq data, using an FDR-corrected *P* value of 0.05, revealed 73 differentially expressed (DE) (>1.3-fold difference) genes between the two molecularly defined subgroups, (Fig. 1*E*). Among the most DE genes, E2F1^{high} samples displayed significant alterations in TNFSF factors including *TNFSF10* (*TRAIL*) and *TNFRSF25* (*DR3*) (Fig. 1*F* and *G*, respectively), previously linked to adipocyte and macrophage dysfunction (24–28). We validated the association between E2F1 and TRAIL or DR3 in an independent cohort (subcohort 2 [Table 2]) of $n = 48$ patients with obesity (Fig. 1*H* and *I*), of whom 11 pairs of patients could also be matched as in our initial analysis (Supplementary Fig. 2). These two analyses largely recapitulated the initial results of the RNA-seq. Moreover, hVAT explants secreted TRAIL proportionally to E2F1 protein expression (Fig. 1*J*). To expand the search for TNFSF that may be enriched among the DE genes based on VAT E2F1 levels, we used the GSEA algorithm (Fig. 1*K*). Among a predefined list of TNFSF members, 19 "leading edge" genes, i.e., TNFSF genes that "crowded" at the top of a ranked list of the entire gene set, were identified. Interestingly, in addition to *TRAIL* and *DR3*, TRAIL receptors *DR4* and *DR5* (*TNFRSF10A/B*) and *TL1A* (*TNFSF15* [ligand for DR3]) emerged as significantly enriched—all but *DR3* more highly expressed in VAT E2F1^{high} compared to VAT E2F1^{low}. Collectively, with use of an unbiased transcriptomic approach, these results uncovered a possible mechanistic link between E2F1 and TNFSF members TRAIL and TL1A in hVAT.

Adipose Tissue Cell Types Expressing TRAIL and TL1A and Their Receptors

The association between E2F1 and TNFSF members suggests that these factors may regulate each other, either directly or indirectly. We initially hypothesized that the TNFSF cytokine TRAIL, which was already shown to alter adipocyte function (26–28), could induce E2F1 expression in adipocytes, the cell fraction in which E2F1 was shown to be upregulated (6). Yet, stimulation of hVAT explants with recombinant hTRAIL did not induce *E2F1* expression (Fig. 2*A*). The plausibility of the reverse regulation—i.e., that E2F1 regulates TRAIL—was supported in human embryonic kidney HEK293 cells, in which overexpression or siRNA-mediated knockdown of E2F1 increased or decreased, respectively, *TRAIL* (Supplementary Fig. 3*A* and *B*). Moreover, possible direct regulation of TRAIL gene expression by E2F1 was proposed by promoter prediction analysis that revealed at least three strong putative E2F1 binding sights in the minimal promoter of hTRAIL (Supplementary Fig. 3*C*). Between these two E2F1-associated TNFSF members, TRAIL dose dependently increased *TRAIL* and *TL1A* mRNA levels in hVAT explants (Fig. 2*A*), suggesting a possible autoregulatory positive-feedback loop. To further delineate this loop, particularly TRAIL-induced TL1A, and its possible implications in adipose tissue, we assessed whether these TNFSF members and their respective receptors similarly originate from the adipocyte and/or the SVF. Following collagenase digestion of hVAT, the adipocyte cell fraction expectedly expressed 200-fold more adiponectin (*ADIPOQ*) and only 15% the *CD68* level compared with SVF, confirming a satisfactory fractions separation (Fig. 2*B*). Quantitative (q)RT-PCR analysis revealed that while *TRAIL* originated from both tissue fractions, *TL1A* was almost exclusively expressed in SVF (Fig. 2*C* and *D*). Interestingly, SVF *TL1A* expression correlated only with adipocyte *TRAIL* ($R^2 = 0.66$, $P = 0.048$) (Fig. 2*E*), not with SVF *TRAIL* ($R^2 = 0.21$, $P = 0.35$), suggesting that TRAIL derived from adipocytes may regulate SVF TL1A. *DR3* (TL1A receptor) and *DR4* and *DR5* (TRAIL receptors) were detectable in both fractions, though significantly more so in SVF (Fig. 2*F*).

To uncover which specific SVF cell type responded to TRAIL by increasing TL1A expression, we first used human peripheral blood mononuclear cells (PBMC). Unpolarized (M0), M1-polarized, or M2-polarized human MDM did not exhibit TRAIL-induced *TL1A* upregulation (Fig. 2*G*). Similarly, for better representation of human adipose tissue macrophages (ATM), MDM differentiated into macrophages in the presence of hVAT-conditioned media were generated, and they, too, did not significantly increase *TL1A* expression in response to hTRAIL stimulation (Supplementary Fig. 3*D*). In contrast to MDM, T cells isolated from the CD14$^-$ cell population of PBMC exhibited dose-dependent hTRAIL-induced *TL1A* (Fig. 2*G*). Additionally, TRAIL treatment augmented TRAIL receptor (*DR4*/*DR5*) expression in T cells (Supplementary Fig. 4). These findings in PBMC-derived cells prompted us to test TL1A induction by TRAIL in bona fide ATM and hVAT T cells. SVF cells isolated from hVAT were stimulated with hTRAIL, stained for cell-specific markers and TL1A protein, and assessed by flow cytometry. Consistent with the PBMC-derived cells, while CD14$^+$ ATM did not exhibit TRAIL-induced TL1A upregulation, adipose tissue CD3$^+$ T cells did (Fig. 2*H* and *I*). Furthermore, this response was apparent in all CD4/CD8 subtypes of adipose tissue T cells—in particular, the double-positive cells (Fig. 2*J*), a subpopulation of T cells shown to be particularly cytokine secreting (29). Thus, adipose tissue T cells, but not ATM, likely contribute to TRAIL-induced TL1A in VAT.

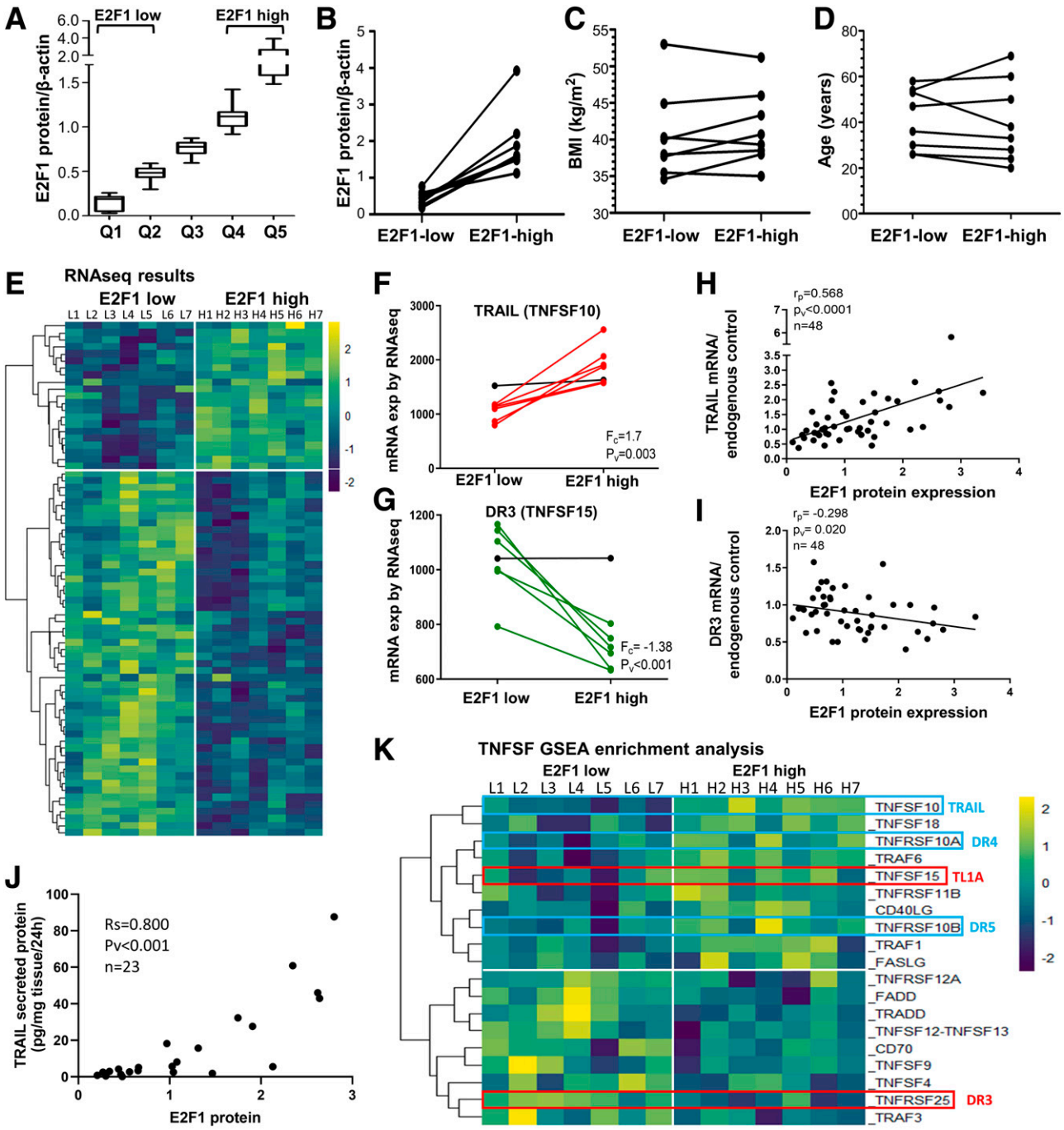

Figure 1— VATs expressing low vs. high E2F1 protein levels display differential transcriptome enriched in TNFSF genes. *A*: E2F1 protein was measured in hVAT samples from $n = 67$ patients to estimate the range of adipose E2F1 protein levels. E2F1 protein levels corresponding to those expressing the lowest vs. highest 40% (quintiles Q1–2 vs. Q4–5, respectively) were designated E2F1^{low} vs. E2F1^{high}. *B–D*: Eight BMI-, age-, and sex-matched pairs were identified (subcohort 1 [Table 2]). *E*: RNA-seq data paired analysis using FDR correction revealed 73 DE genes (fold change >1.3, $P \leq 0.05$) among seven matched pairs (i.e., $n = 14$ persons) of VAT E2F1$^{low/high}$ (one pair had to be excluded [RESEARCH DESIGN AND METHODS]). Hierarchical clustering was done using the heat map function in R. *F* and *G*: RNA-seq results for *TRAIL* (*TNFSF10*) and *DR3* (*TNFRSF25*), respectively. Red lines, >10% increase in E2F1; green lines, >10% decrease in E2F1; black lines, <10% change in E2F1 expression (exp). *H* and *I*: Validation of RNA-seq results was done for *TRAIL* and *DR3* by Pearson correlation analysis with VAT E2F1 protein in an independent, larger nonmatched cohort ($n = 48$) (subcohort 2 [Table 2]). *J*: Secretion of TRAIL to the media by hVAT explants (Spearman rank correlation). *K*: GSEA enrichment analysis of the entire RNA-seq data against a list of TNFSF members. Shown is the hierarchical clustering of the top 19 "leading edge" members, including *TRAIL* (*TNFSF10*) and *TL1A* (*TNFSF15*) and their respective receptors: *DR4/5* (*TNFRSF10A/B*) and *DR3* (*TNFRSF25*).

Table 2—Clinical characteristics of participants from the Beer-Sheva subcohorts from the Beer-Sheva biobank

	Subcohort 1, matched pairs	Subcohort 2, validation	Subcohort 3, patients with diabetes vs. patients without diabetes	Subcohort 4, ATM lipid accumulaion
n	16 (8 matched pairs)	48 (including 11 matched pairs)	35	24
Age (years)	40.75 ± 8.9	40.7 ± 11	38.7 ± 10.1	41.2 ± 14.5
Sex (% female)	62	64	68	58
BMI (kg/m^2)	41.6 ± 5	41.9 ± 9	41.2 ± 3.7	34.7 ± 6.1*
FPG (mg/dL)	97 ± 22	116.85 ± 39	116.6 ± 29	94 ± 32
TG (mg/dL)	158.8 ± 65.8	150.76 ± 63	144 ± 42	159 ± 59
LDL (mg/dL)	116.5 ± 28	125.2 ± 30	114.5 ± 24	103.2 ± 22
HDL (mg/dL)	41.6 ± 8.7	42.1 ± 6.2	42.3 ± 9	40 ± 14.5
Systolic BP (mmHg)	146 ± 17	139.1 ± 20	139 ± 12.3	124.2 ± 13.07

Values are means ± SD. Participants in the subcohorts are not overlapping. Studies 1–3 include patients with obesity (i.e., BMI ≥30 kg/m^2). *This study included participants with overweight (i.e., BMI ≥25 kg/m^2). BP, blood pressure. FPG, fasting plasma glucose.

Functional Impact of TL1A in Adipocytes and Macrophages

TL1A Induces Insulin Resistance and Secretory Malfunction in Human Adipocytes

Possible contribution of TRAIL to adipose tissue dysfunction in obesity has previously been reported (26). Given our results so far, we assessed whether this could be mediated by TL1A. We used Chub-S7, a human preadipocyte cell line that readily differentiates into adipocyte-like cells (Supplementary Fig. 1). First, given the proapoptotic action of many TNFSF factors, we verified that TL1A (up to 25 ng/mL) did not increase adipocyte cell death (Fig. 3*A*). Human Chub-S7 adipocytes treated for 24 h with hTL1A dose dependently decreased adiponectin and increased leptin secretion, resulting in significantly reduced secreted adiponectin-to-leptin ratio (Fig. 3*B–D*). Additionally, TL1A-treated cells exhibited a significantly attenuated insulin-stimulated Akt and GSK phosphorylation, suggesting induction of insulin resistance (Fig. 3*E–G*). Indeed, metabolically, TL1A pretreatment stimulated basal lipolysis and perturbed the capacity of insulin to inhibit isoproterenol-stimulated lipolysis (Fig. 3*H*). Finally, human adipocytes treated with TL1A exhibited increased expression of *E2F1* mRNA (Fig. 3*I*), albeit non-dose-dependently. This suggests that TL1A, even at low doses, may contribute to elevated adipose tissue E2F1 expression in human obesity. Collectively, TL1A, possibly released by T-cells in E2F1^{high} VAT, can induce adipocyte dysfunction without increasing adipocyte cell death and possibly fuels a vicious cycle by contributing to a VAT milieu that upregulates adipocyte E2F1.

TL1A Induces Macrophage Polarization and Lipid Accumulation

ATM are thought to contribute to whole adipose tissue dysfunction in obesity, specifically when displaying a proinflammatory profile and becoming lipid laden (15,30). Interestingly, TL1A was previously reported to support macrophage proinflammatory activation, cholesterol accumulation, and foam cells formation (24), without increasing cell death. Consistently, human MDM exhibited increased neutral-lipid accumulation following 24 h exposure to hTL1A—interestingly, more so in the absence (~3.5-fold) than in the presence (25% increase) of oleic acid added to the media (Fig. 4*A* and *B*, respectively). The greater effect in the absence of oleic acid suggests that TL1A supports de novo lipogenesis (Fig. 4*C*). This was supported by the finding that C75, a fatty-acyl synthase (FASN) inhibitor, significantly inhibited (by ~75%) TL1A-induced lipid accumulation in MDM in the absence, but not in the presence, of oleic acid (Fig. 4*D*). Inhibitors of steps common to both de novo lipogenesis and fatty acid reesterification (Fig. 4*C*) invariably inhibited TL1A-induced lipid accumulation in MDM (Fig. 4*D*). Complementarily, TL1A induced the expression of glucose transporter *GLUT1* and *FASN* and *DGAT1* but not of the lipid transporter *CD36* (Fig. 4*E*). These data suggest that TL1A's induction of de novo lipogenesis is mediated via upregulation of both exclusive de novo lipogenic (FASN) and common enzymes to fatty acid reesterification. Moreover, TL1A may rely on these two lipogenic pathways in macrophages depending on the availability of fatty acids.

Additionally, in human MDM, TL1A induced increased mRNA levels of typical M1-polarization genes (IL6, MCP1) (Fig. 5*A*) and lower M2 markers (CD206, CD209) (Fig. 5*B*). Lastly, we assessed whether TL1A-prestimulated macrophages may induce adipocyte dysfunction: human MDM pretreated for 24 h with TL1A were washed and cocultured with human adipocytes (Fig. 5*C*) and induced decreased adiponectin-to-leptin ratio in the adipocyte conditioned media (Fig. 5*D*). Jointly, in human macrophages, TL1A induces lipid accumulation, supports a proinflammatory profile, and disrupts macrophage-adipocyte communication as evident by a dysfunctional adipocyte secretory profile.

Potential Clinical Significance of Elevated TL1A in VAT

Using expression data from our Beer-Sheva cohort of patients with obesity, we observed that VAT expression of

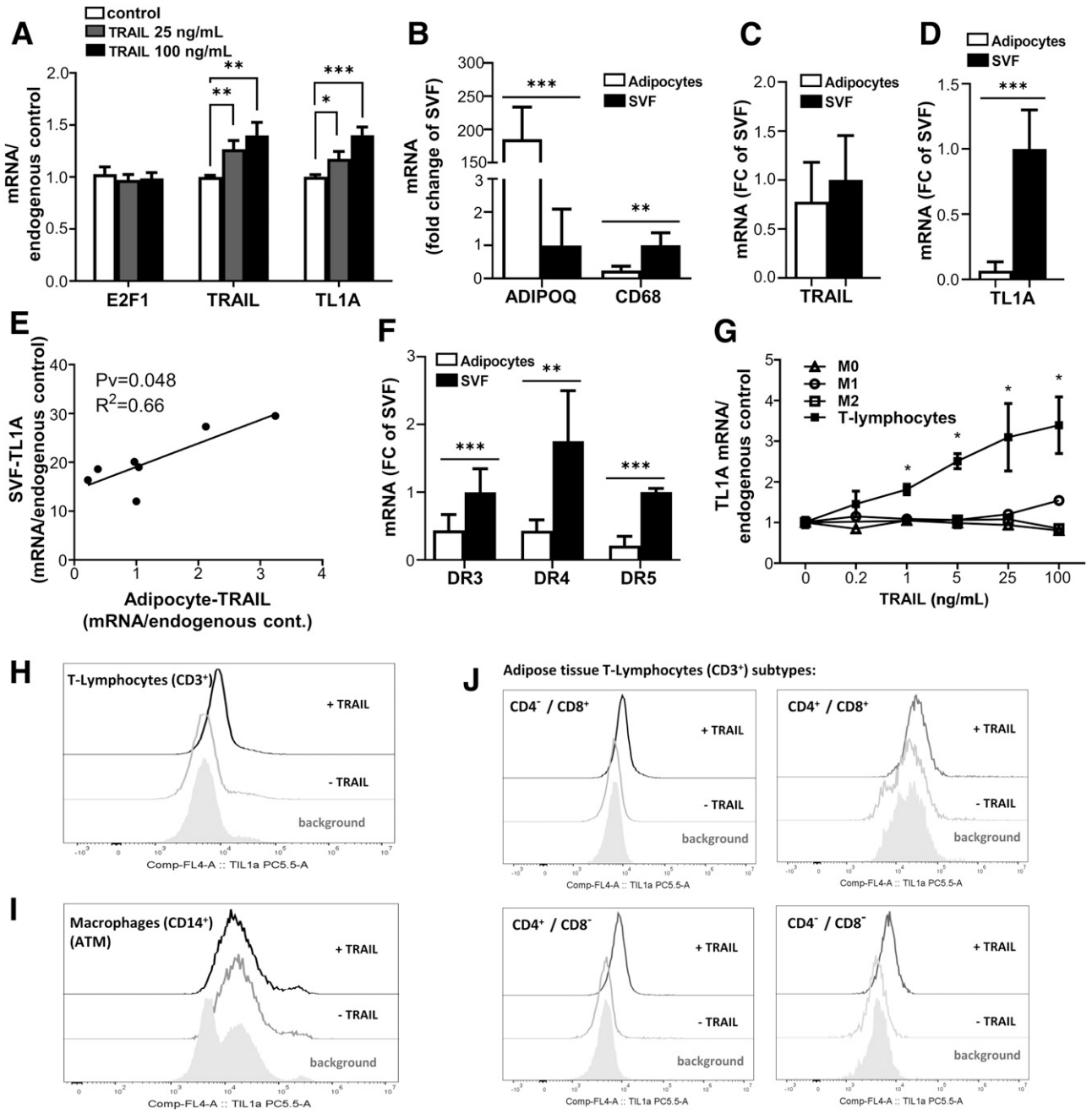

Figure 2—TRAIL-induced TL1A expression is attributed to human visceral fat T cells. *A*: hVAT explants were cultured ex vivo (24 h) with hTRAIL at increasing concentrations, and mRNA expression of *E2F1*, *TRAIL*, and *TL1A* in the explants was measured by qRT-PCR (results are mean ± SD of three experiments, each with three biological replicates and two technical replicates). *B*: VAT explants were fractionated to adipocytes and SVF using collagenase digestion. Efficient fractionation was validated by *CD68* vs. *ADIPOQ* expression as markers of the SVF and adipocyte fractions, respectively, using qRT-PCR ($n = 7$ samples in technical duplicates). *C* and *D*: Expression of *TRAIL* and *TL1A* in the adipocyte and SVF fractions was assessed using qRT-PCR ($n = 7$ samples in technical duplicates). *E*: Spearman correlation between adipocyte fraction *TRAIL* expression and SVF expression of *TL1A*. *F*: Expression of *DR4*, *DR5* (TRAIL receptors), and *DR3* (TL1A receptor) in hVAT adipocyte and SVF fractions assessed using qRT-PCR ($n = 7$ samples in technical duplicates). *G*: Human MDM were either kept unpolarized (M0), or polarized to classical M1 or M2 phenotypes. $CD3^+$ lymphocytes were isolated from the $CD14^-$ cells as described in RESEARCH DESIGN AND METHODS. Cultured cells were stimulated with hTRAIL at the indicated concentrations for 24 h, and the expression of *TL1A* mRNA was measured by qRT-PCR (results are mean ± SD of two experiments, each with three biological replicates and two technical replicates). All mRNA results are presented as mRNA/endogenous control (*PPIA*, *PGK1*) using *ddCT* (delta delta CT). *H* and *I*: SVF from hVAT was stimulated (or not) with hTRAIL, then stained for T cells (anti-CD3 Ab) or macrophages (anti-CD14 Ab), and for TL1A, and analyzed by FACS, as detailed in RESEARCH DESIGN AND METHODS. *J*: CD4/CD8 subclasses of the $CD3^+$ adipose tissue T lymphocytes were identified by staining with the respective antibodies, along with anti-TL1A Ab, and analyzed by FACS. cont., control; FC, fold change.

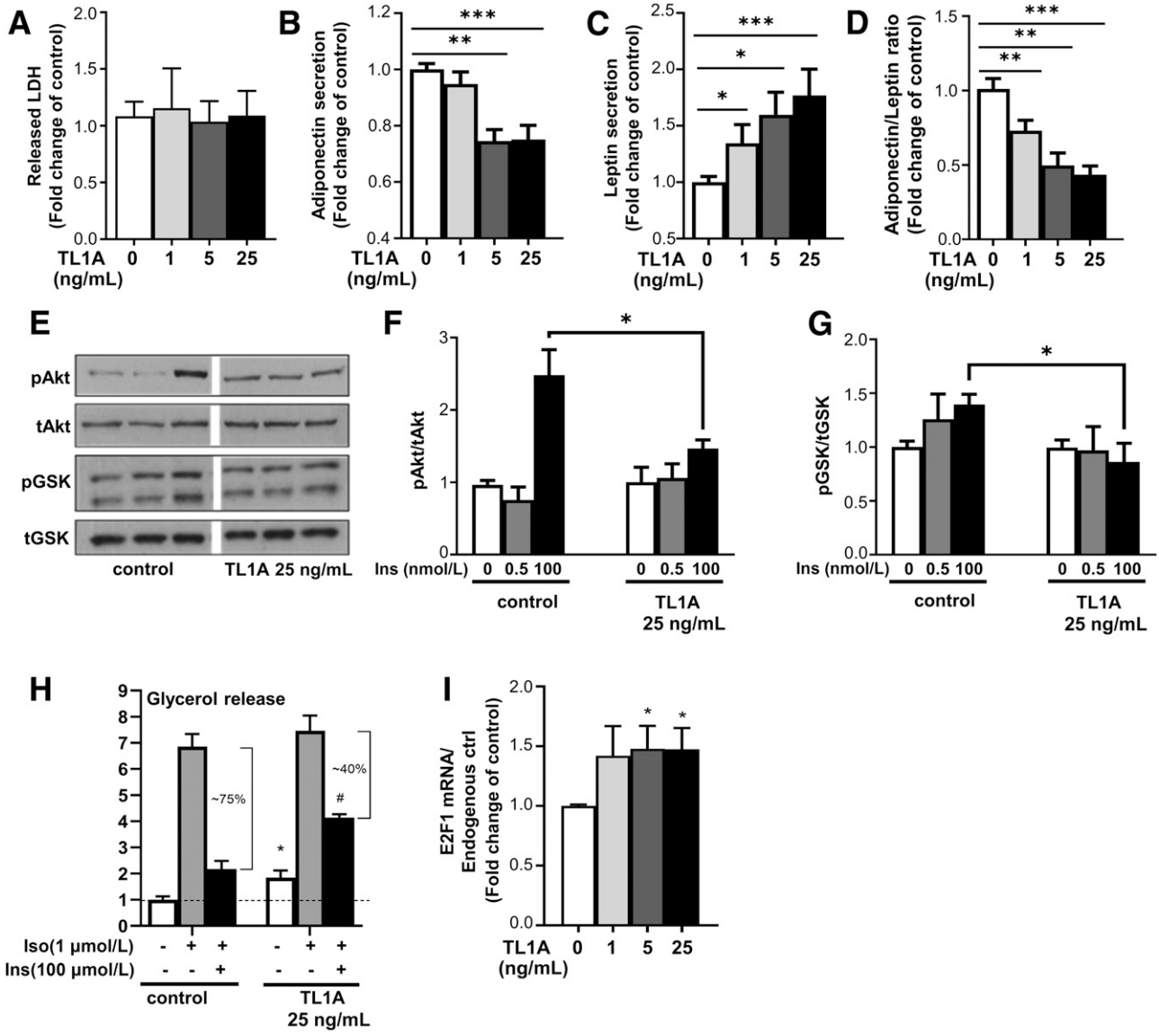

Figure 3—TL1A induces metabolic and endocrine dysfunction in human adipocytes. Differentiated human Chub-S7 adipocytes were stimulated with the indicated concentrations of hTL1A for 24 h, and LDH release to conditioned media was measured (results are presented as media LDH/total LDH) (mean ± SEM of two experiments, each with three biological replicates and two technical replicates) (*A*). Secretion of adiponectin (*B*) and leptin (*C*) was measured in the media (two experiments, each with biological and technical duplicates), and adiponectin-to-leptin ratio was calculated (*D*). *E*: Cells were stimulated for 24 h with hTL1A 25 ng/mL, washed, and stimulated acutely (7 min) with the indicated insulin concentrations. Cell lysates were assessed for phosphorylated (p)Akt, total (t)Akt, phosphorylated GSK3, and total GSK3 (blots presented are different parts of a single gel, and splicing of the image was to enhance clarity of the presentation). Densitometry of blots from three independent experiments (each with biological duplicates) is shown in *F* and *G*. *H*: hTL1A-treated and control adipocytes were stimulated with 1 µmol/L isoproterenol (Iso) without or with 100 nmol/L insulin (Ins), and glycerol release to the media was measured. Results are presented as fold of basal glycerol release (two independent experiments, each with three biological and two technical replicates). *I*: *E2F1* mRNA levels in Chub-S7 adipocytes incubated with the indicated concentrations of hTL1A for 24 h were measured by qRT-PCR (two experiments with two biological and two technical replicates). Results are presented as mRNA/endogenous control (*PPIA*, *PGK1*) using *ddCT* (mean ± SEM). ctrl, control.

TL1A, *TRAIL*, and *E2F1* was significantly higher in those whose obesity was complicated by type 2 diabetes (T2D) than in those without diabetes (subcohort 3 [Fig. 6*A*–*C*]). Moreover, patients with high ATM lipid content expressed higher *TL1A* and *TRAIL* mRNA in whole VAT (subcohort 4 [Fig. 6*D* and *E*]). In addition, using the Leipzig cohort ($n = 421$, all with BMI $\geq$30 kg/m^2) (Table 1), we found that the expression of most of the TNFSF members studied herein significantly intercorrelated (Fig. 6*F*), with the strongest correlation observed between *TRAIL* and *TL1A* ($r = 0.646$, $P < 0.001$), consistent with the proposition that TRAIL regulates *TL1A* expression. We then divided the cohort population into subgroups based on low (lower two quintiles, i.e., lower 40%) or high (upper two quintiles,

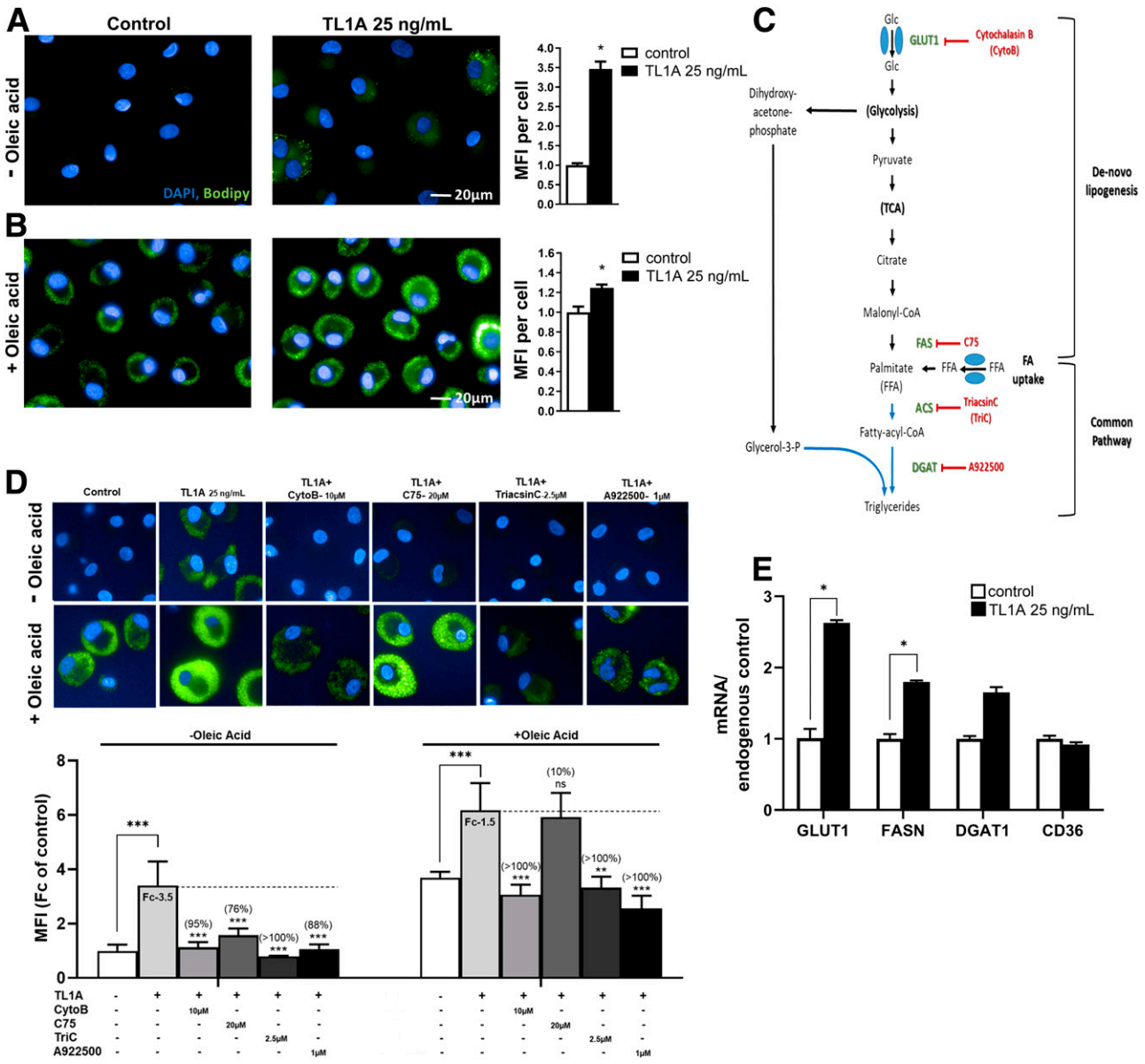

Figure 4— TL1A induces lipid accumulation in human macrophages. Human circulating monocytes were isolated using CD14 beads, cultured in vitro, and differentiated into macrophages over 6 days (MDM). Cells were treated with hTL1A 25 ng/mL for 24 h in the absence (*A*) or presence (*B*) of oleic acid (100 nmol/L), fixed, and incubated with DAPI and BODIPY to stain nuclei (blue) and neutral lipids (green), respectively. Intracellular lipid quantification was conducted using high-throughput microscopy (Operetta); results are mean ± SEM of two experiments, each with three biological replicates. Images are representative parts of Operetta files. MFI, mean fluorescence intensity. *C*: Metabolic pathways of lipogenesis—de novo lipogenesis and fatty acid uptake and esterification—and inhibitors used to uncover pathways used by TL1A to stimulate lipid accumulation in MDM. *D*: Human MDM were treated as in *A* and *B*, without or with the indicated inhibitors. Shown are representative images of five independent experiments (two for +oleic acid), each performed in triplicates, and BODIPY mean fluorescence intensity quantification is shown in the graphs below. Percentage of inhibition of TL1A-induced lipogenesis is shown in parentheses. *E*: MDM treated with hTL1A were analyzed for mRNA expression of *GLUT1*, *FASN*, *DGAT1*, or *CD36* using qRT-PCR. Results are presented as mRNA/endogenous control (*PPIA*, *PGK1*) (*ddCT*) (mean ± SEM of two to four experiments, each with three biological replicates and two technical replicates). *$P \leq 0.05$; **$P \leq 0.01$; ***$P \leq 0.001$. Fc, fold change.

i.e., upper 40%) *TRAIL* and *TL1A* expression, consistent with our approach for E2F1 (Fig. 1*A*). This generated four *TRAIL/TL1A* expression groups: low-low/low-high/high-low/high-high. Since the high-low and low-high groups were very small ($n = 16$ and $n = 20$, respectively), we compared the two extreme groups (high-high vs. low-low, $n = 142$ and $n = 148$, respectively). There were no significant differences in mean age, sex, or BMI between the groups (Fig. 6*G*). Yet, the high-high group exhibited significantly higher serum IL6 and leptin levels. Jointly, these analyses support the putative contribution of E2F1-related TNFSF members to adipose tissue dysfunction in human obesity.

DISCUSSION

Previous studies established a non-cell-cycle role for E2F1 in VAT, driving the expression of autophagy and a MAPK

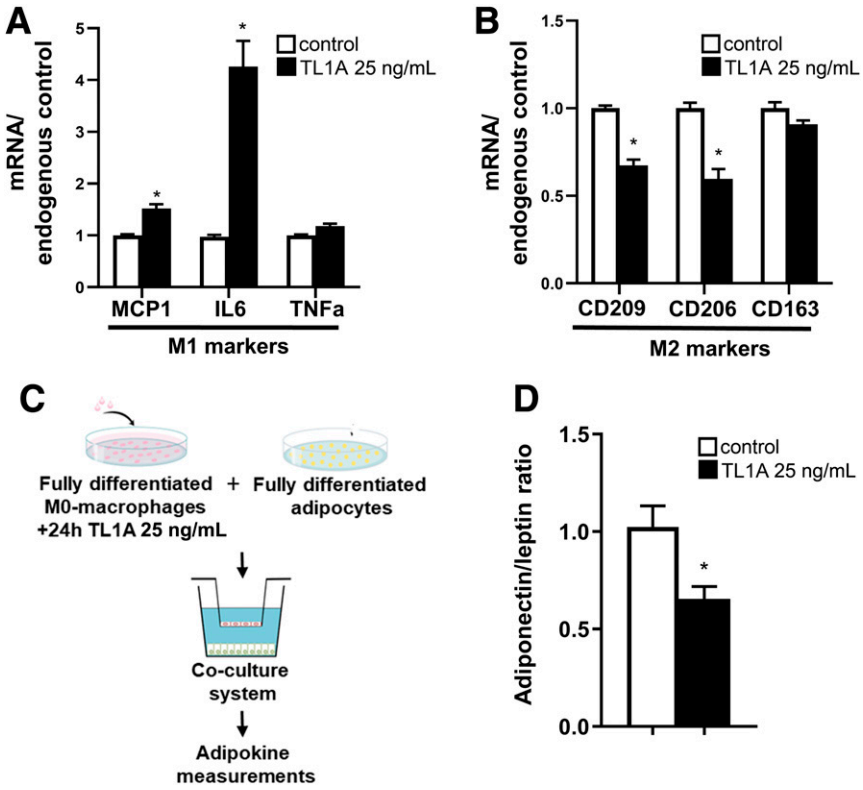

Figure 5—TL1A induces macrophages M1/M2 polarization shift and macrophage-mediated human adipocyte secretory dysfunction. *A* and *B*: Human MDM were treated with hTL1A for 24 h, and marker genes for M1 and M2 polarization were measured using qRT-PCR. Results are presented as mRNA/endogenous control (*PPIA*, *PGK1*) (*ddCT*) (mean ± SEM of two experiments, each with three biological replicates and two technical replicates). *C*: Human MDM were cultured and differentiated on 0.4 μm high-pore-density inserts. Inserts were then incubated for 24 h with or without hTL1A 25 ng/mL, washed, and transferred to plates containing mature human Chub-S7 adipocytes. Conditioned media was collected, and secreted adiponectin and leptin were measured by ELISA. Adiponectin-to-leptin ratio was calculated (*D*). (Results are from two experiments, each performed with three biological replicates and two technical replicates.) *$P < 0.05$.

cascade, two stress pathways through which E2F1 contributes to adipose tissue dysfunction in obesity (5,6). In the current study, we used an unbiased approach to uncover additional mechanisms/mediators that could connect high expression of VAT E2F1 in human obesity with increased cardiometabolic risk. Indeed, E2F1^{high} VAT expressed a distinct transcriptome compared with E2F1^{low} VAT, independently of age, sex, and the degree of obesity, including differential expression of multiple TNFSF members. Expression of *TRAIL* (*TNFSF10*) and *TL1A* (*TNFSF15*) was enriched in patients with obesity and E2F1^{high} VAT, TRAIL secretion by hVAT was proportional to E2F1 expression, and tissue fractionation suggested that while TRAIL originates from both adipocytes and SVF, TL1A is predominantly expressed in SVF. TRAIL treatment of whole adipose tissue induced upregulation of both *TRAIL* itself and *TL1A*, the latter originating from VAT T cells. Since the expression of *TL1A* in SVF correlated only with *TRAIL* expression in VAT adipocyte fraction (but not SVF), we propose the following model (Fig. 7): Upregulated adipocyte E2F1 induces TRAIL, which in turn upregulates TL1A in adipose tissue T cells. Elevated VAT TL1A induces ATM inflammatory polarization and lipid accumulation and in adipocytes disrupt insulin responsiveness, lipolysis, and adipokine secretory profile (the latter both directly and via TL1A's effect on ATM). Furthermore, elevated VAT TL1A may further contribute to upregulate adipocyte *E2F1* expression, thereby completing a vicious-cycle regulatory loop. This putative E2F1-associated TRAIL-TL1A loop is likely clinically relevant, as VAT *TL1A* strongly correlated with that of *TRAIL* and the TNFSF receptors in a large human cohort of $n = 421$ patients. *TL1A* also significantly associated with circulating IL-6 and leptin levels and was elevated in those with T2D and in patients with increased ATM lipid content.

TNFα, the best-characterized TNFSF cytokine, was the first inflammatory mediator implicated in the development of adipose tissue and systemic insulin resistance in obesity (31), followed by Fas ligand and additional members (32,33). Interestingly, despite structural and functional resemblance, TNFSF members activate distinct molecular mechanisms. TRAIL was previously identified as a major effector of adipocyte function and systemic metabolic status (27,28). In preadipocytes, TRAIL exerts a proliferative effect and may thus support hyperplastic adipose tissue expansion when upregulated in obesity (34). Yet, TRAIL was also

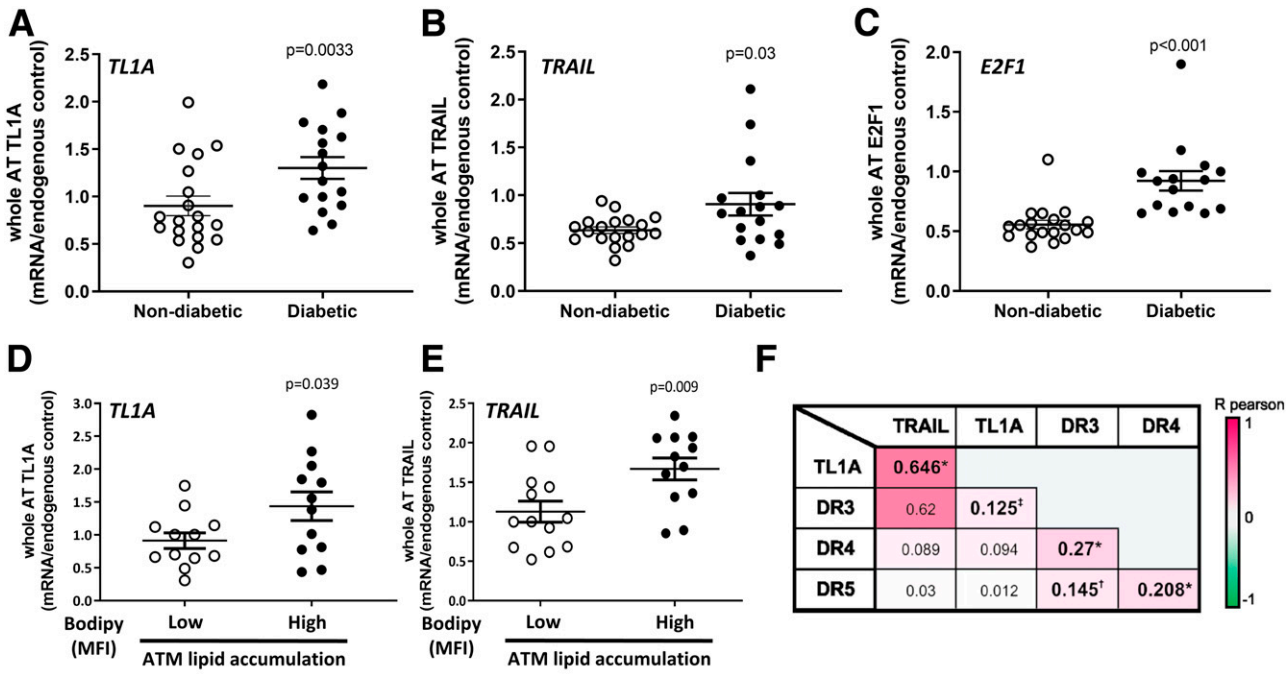

G

	TRAIL_TL1A low	TRAIL_TL1A high	p value
N	n=148	n=142	
hVAT-TL1A mRNA (AU)	0.29±0.12	1.22±0.41	**<0.001**
hVAT-TRAIL mRNA (AU)	0.30±0.13	1.23±0.37	**<0.001**
Age (y)	46.7±11.5	45.9±10.4	0.563
Sex (% female)	70%	81%	
BMI (kg/m^2)	48.3±8.3	50.3±10.3	0.063
FFA (serum, mmol/L)	0.8±0.4	0.9±0.5	0.180
Adiponectin (serum, µg/ml)	7.6±5.8	8.1±7	0.522
Leptin (serum, ng/ml)	49.1±21.9	55.7±20.6	**0.030**
IL6 (serum, ng/ml)	5.5±3.2	9.1±5.9	**0.020**

Figure 6—Potential clinical significance of elevated *TL1A* and *TRAIL* in hVAT. *A–C*: *TL1A, TRAIL*, and *E2F1* mRNA expression was measured in hVAT of obese patients without or with T2D of the Beer-Sheva cohort ($n = 35$) (subcohort 3 [see Table 2]) using qRT-PCR. Differential expression was tested using Mann-Whitney test. *D* and *E*: hVAT samples were subjected to collagenase digestion ($n = 24$) (subcohort 4 [see Table 2]), ATMs were sorted based on surface markers using FACS analysis, and their lipid content was assessed by BODIPY fluorescence. Patients were categorized as having "high" or "low" ATM lipid content based on being above vs. below median mean fluorescence intensity (MFI), respectively. mRNA expression of *TL1A* and *TRAIL* in the respective whole tissue samples was compared between the groups of high- and low-lipid-laden macrophages. mRNA levels were measured by qRT-PCR, and differential expression between the groups was tested by Mann-Whitney test. Results are displayed as mean ± SEM. *F*: mRNA expression levels of *TL1A*, *TRAIL*, and the corresponding receptors *DR3*, *DR4*, and *DR5* were measured in hVAT of the Leipzig cohort ($n = 421$) (see Table 1) using qRT-PCR. Correlations between the different genes were evaluated by Pearson parametric correlation test using SPSS Statistics. Pearson *r* of the correlation is represented by color scale: red, positive correlation; green, negative correlation. *Significance with P of <0.001; †significance with $P = 0.01$; ‡significance with $P = 0.05$. *G*: Clinical characteristics of patients with combined low vs. high *TRAIL-TL1A* in hVAT. The Leipzig cohort population was divided into quintiles of both *TRAIL* and *TL1A* expression, and *TL1A* high vs. low as well as *TRAIL* high vs. low groups were defined based on upper and lower 40% of the population, respectively. The two parameters were intersected to create a four-group categorization method of TL1A_TRAIL index, and the two extreme subgroups (low/low, $n = 148$, vs. high/high, $n = 142$) were compared for clinical parameters. Means ± SD were compared by nonmatched *t* test using SPSS Statistics. AT, adipose tissue; AU, arbitrary units; y, years.

shown to inhibit early adipogenesis (28), which may contribute to hypertrophic adipose tissue expansion, and to facilitate an inflammatory transcriptome in preadipocytes (16). In mature adipocytes, TRAIL also induced an inflammatory profile (16), while impairing insulin response (27). These effects were all mediated by the proapoptotic DR4 and DR5 receptors but were not accompanied by increased apoptosis (28), demonstrating that "death

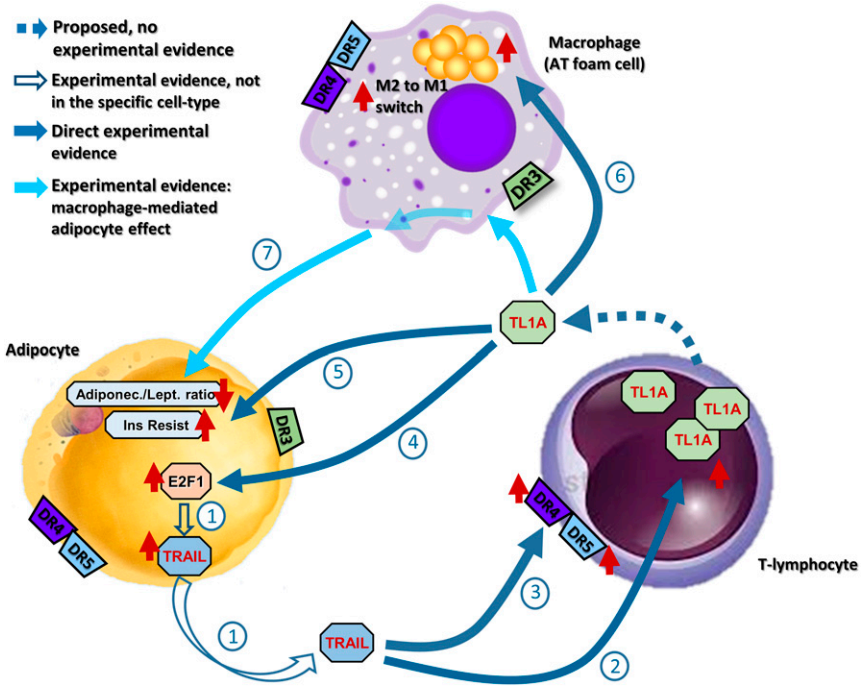

Figure 7—A proposed tripartite paracrine TNFSF network involving adipocytes, lymphocytes, and macrophages in adipose tissue. E2F1-mediated overexpression of TRAIL (TNFSF10), particularly in adipocytes (circle 1) (Supplementary Fig. 3*A–C*), increases the secretion of TRAIL (circle 1) (Fig. 1*J*). Adipose tissue T cells upregulate TL1A (TFFSF15) in response to TRAIL (circle 2) (Fig. 2*G–J*) and increase DR4/DR5 expression (circle 3 [Supplementary Fig. 4]). Lymphocyte-derived TL1A upregulates adipocyte E2F1 (circle 4) (Fig. 3*I*), impairs adipocyte insulin signaling and antilipolytic action (circle 5) (Fig. 3*E–H*), and induces an adverse adipokine secretory phenotype (circle 5) (Fig. 3*B–D*). In parallel, TL1A induces lipid accumulation in macrophages (circle 6) (Fig. 4) and supports their proinflammatory phenotype (circle 6) (Fig. 5*A* and *B*). Finally, mediated by macrophages, TL1A induces an adipocyte adverse adipokine secretory phenotype (circle 7) (Fig. 5*C* and *D*). AT, adipose tissue.

receptor" signaling activates, at least in adipocytes, nonapoptotic pathways. In macrophages, TRAIL promotes cytokine production (35) and regulates macrophage autophagy (36), a process known to be altered in diseased adipose tissue and specifically in ATM (23,37). TRAIL also induces the formation of lipid-laden foam cells (25), though these were cholesterol-accumulating macrophages rather than the triglyceride (TG)-filled ones found in obese adipose tissue. Jointly, at the cellular level, current literature supports a putative role for TRAIL in driving dysfunctional cell phenotypes, which could promote adipose tissue dysfunction in obesity. Systemically, the effects of TRAIL are more complex. Serum levels of TRAIL in human patients correlate with total body fat, weight gain, and circulating cholesterol levels (reviewed in 26), and mouse models of genetic obesity show elevated expression of *TRAIL* and its receptors in adipose tissue (27). Serum TRAIL is interestingly lower in patients newly diagnosed with T2D but is elevated in patients with severe end-organ complications (26). Within the subpopulation of T2D patients, TRAIL presents significant correlations with BMI, TGs, and HOMA of insulin resistance, suggesting it as a marker for disease severity. Conversely, in different animal models it has been suggested that administering TRAIL can decrease lipid accumulation and proinflammatory activation in adipose tissue and even improve insulin sensitivity (38). Curiously, similar discrepancies in pathogenic versus protective roles of TRAIL were demonstrated in atherosclerosis (reviewed in 39) and in cancer (40). Altogether, though signaling via death receptors, TRAIL serves as a mediator of multiple biological nonapoptotic processes. Its pathogenic effect in adipose tissue is complex and might be imposed on adipocytes both directly and indirectly via other cell types, as suggested herein.

TL1A, another well-characterized TNFSF, has mostly been studied for its involvement in inflammatory and autoimmune diseases but has only recently been implicated in obesity (41). We found increased *TL1A* expression in adipose tissue in a TRAIL-dependent manner, consistent with TRAIL-TL1A coupling, as was previously shown in skin lesions of patients with diabetes (42). Additionally, involvement of TL1A in a TNFSF feed-forward loop has been proposed before in the pathogenesis of rheumatoid arthritis, in which TL1A induced elevated TNFα (and IL17) levels (43). Classically, TL1A is mainly known as a lymphocyte-driven cytokine that stimulates T and B cells (17), directing their polarization and thus modulating immune responses (44,45). TL1A's expression in T cells is induced upon diverse inflammatory stimuli, though to our knowledge TRAIL was not implicated before. A putative central role for TL1A in autoimmunity is exemplified in inflammatory bowel disease (45), rheumatoid arthritis (46),

psoriasis (43), primary sclerosing cholangitis (43), ankylosing spondylitis (47), and even airway hyperreactivity diseases (48), all of which are associated with elevated levels of both disease-site and circulating TL1A. Studies in animal models support a central mediatory role of TL1A by demonstrating that deletion/blockade of either TL1A or DR3 resulted in reduced disease severity (43,48). In obesity, also a chronic inflammatory disease, TL1A may serve as a previously unrecognized central pathogenic player. Herein, we suggest that TL1A may function as a paracrine mediator of lymphocyte-macrophage, lymphocyte-adipocytes, and lymphocyte-macrophage-adipocytes communication within adipose tissue (Fig. 7).

In conclusion, we describe a complex paracrine network of TNFSF factors in adipose tissue in a high-risk obesity subphenotype characterized by high E2F1 expression. Our model, tying E2F1, TRAIL, and TL1A in a single pathophysiological path, expands understanding of both E2F1 and TRAIL activity, each previously shown to induce adipose tissue dysfunction, and highlights the complexity and importance of TNFSF cytokines in the pathophysiology of adipose tissue. Also, our study proposes that when elevated in a subgroup of patients with obesity, TL1A is a mediator of adipose tissue and whole-body metabolic dysfunction. Our results suggest new therapeutic opportunities in the quest for a more precision/personalized approach to better manage the cardiometabolic complications of molecularly defined obesity subphenotypes.

Funding. This study was supported in part by grants from Deutsche Forschungsgemeinschaft (DFG) (German Research Foundation), 209933838 project number SFB1052: "Obesity mechanisms," and the Israel Science Foundation (ISF 2176/19).

Duality of Interest. No potential conflicts of interest relevant to this article were reported.

Author Contributions. N.M. conducted experiments and wrote the manuscript. T.P. conducted experiments and reviewed the data. Y.H. developed experimental methods. V.C.-C. conducted bioinformatic analyses. N.G. reviewed the data and manuscript. T.T. conducted experiments. I.F.L. helped establish the human Beer-Sheva cohort. B.K. helped establish the human Beer-Sheva cohort and obtained tissue biopsies. R.G. helped in epidemiological analyses of human data. O.B. and A.M. conducted flow cytometry analyses. N.B. reviewed the data and manuscript. M.B. established and provided the human Leipzig cohort, reviewed the data, and edited the manuscript. A.R. supervised the research and wrote the manuscript. A.R. and N.M. are the guarantors of this work and, as such, had full access to all the data in the study and take responsibility for the integrity of the data and the accuracy of the data analysis.

References

1. Kyle TK, Dhurandhar EJ, Allison DB. Regarding obesity as a disease: evolving policies and their implications. Endocrinol Metab Clin North Am 2016; 45:511–520

2. Piché ME, Tchernof A, Després JP. Obesity phenotypes, diabetes, and cardiovascular diseases. Circ Res 2020;126:1477–1500

3. Samocha-Bonet D, Chisholm DJ, Tonks K, Campbell LV, Greenfield JR. Insulin-sensitive obesity in humans - a 'favorable fat' phenotype? Trends Endocrinol Metab 2012;23:116–124

4. Bel Lassen P, Charlotte F, Liu Y, et al. The FAT score, a fibrosis score of adipose tissue: predicting weight-loss outcome after gastric bypass. J Clin Endocrinol Metab 2017;102:2443–2453

5. Haim Y, Blüher M, Konrad D, et al. ASK1 (MAP3K5) is transcriptionally upregulated by E2F1 in adipose tissue in obesity, molecularly defining a human dys-metabolic obese phenotype. Mol Metab 2017;6:725–736

6. Haim Y, Blüher M, Slutsky N, et al. Elevated autophagy gene expression in adipose tissue of obese humans: a potential non-cell-cycle-dependent function of E2F1. Autophagy 2015;11:2074–2088

7. Fajas L, Landsberg RL, Huss-Garcia Y, Sardet C, Lees JA, Auwerx J. E2Fs regulate adipocyte differentiation. Dev Cell 2002;3:39–49

8. Blanchet E, Annicotte JS, Lagarrigue S, et al. E2F transcription factor-1 regulates oxidative metabolism. Nat Cell Biol 2011;13:1146–1152

9. Hsieh MC, Das D, Sambandam N, Zhang MQ, Nahlé Z. Regulation of the PDK4 isozyme by the Rb-E2F1 complex. J Biol Chem 2008;283:27410–27417

10. Annicotte JS, Blanchet E, Chavey C, et al. The CDK4-pRB-E2F1 pathway controls insulin secretion. Nat Cell Biol 2009;11:1017–1023

11. Fajas L, Annicotte JS, Miard S, Sarruf D, Watanabe M, Auwerx J. Impaired pancreatic growth, beta cell mass, and beta cell function in E2F1 (-/-)mice. J Clin Invest 2004;113:1288–1295

12. Denechaud PD, Lopez-Mejia IC, Giralt A, et al. E2F1 mediates sustained lipogenesis and contributes to hepatic steatosis. J Clin Invest 2016;126:137–150

13. Giralt A, Denechaud PD, Lopez-Mejia IC, et al. E2F1 promotes hepatic gluconeogenesis and contributes to hyperglycemia during diabetes. Mol Metab 2018;11:104–112

14. Ying L, Marino J, Hussain SP, et al. Chronic inflammation promotes retinoblastoma protein hyperphosphorylation and E2F1 activation. Cancer Res 2005; 65:9132–9136

15. Shapiro H, Pecht T, Shaco-Levy R, et al. Adipose tissue foam cells are present in human obesity. J Clin Endocrinol Metab 2013;98:1173–1181

16. Zoller V, Funcke JB, Roos J, et al. Trail (TNF-related apoptosis-inducing ligand) induces an inflammatory response in human adipocytes. Sci Rep 2017;7: 5691

17. Bamias G, Martin C III, Marini M, et al. Expression, localization, and functional activity of TL1A, a novel Th1-polarizing cytokine in inflammatory bowel disease. J Immunol 2003;171:4868–4874

18. Sklarz MY, Levin L, Gordon M, Chalifa-Caspi V. NeatSeq-Flow: a lightweight high-throughput sequencing workflow platform for non-programmers and programmers alike. 18 December 2018 [preprint]. bioRxiv:173005

19. Dobin A, Davis CA, Schlesinger F, et al. STAR: ultrafast universal RNA-seq aligner. Bioinformatics 2013;29:15–21

20. Li B, Dewey CN. RSEM: accurate transcript quantification from RNA-Seq data with or without a reference genome. BMC Bioinformatics 2011;12:323

21. Love MI, Huber W, Anders S. Moderated estimation of fold change and dispersion for RNA-seq data with DESeq2. Genome Biol 2014;15:550

22. Lee MJ, Fried SK. Glucocorticoids antagonize tumor necrosis factor-α-stimulated lipolysis and resistance to the antilipolytic effect of insulin in human adipocytes. Am J Physiol Endocrinol Metab 2012;303:E1126–E1133

23. Bechor S, Nachmias D, Elia N, et al. Adipose tissue conditioned media support macrophage lipid-droplet biogenesis by interfering with autophagic flux. Biochim Biophys Acta Mol Cell Biol Lipids 2017;1862:1001–1012

24. McLaren JE, Calder CJ, McSharry BP, et al. The TNF-like protein 1A-death receptor 3 pathway promotes macrophage foam cell formation in vitro. J Immunol 2010;184:5827–5834

25. Liu FF, Wu X, Zhang Y, Wang Y, Jiang F. TRAIL/DR5 signaling promotes macrophage foam cell formation by modulating scavenger receptor expression. PLoS One 2014;9:e87059

26. Harith HH, Morris MJ, Kavurma MM. On the TRAIL of obesity and diabetes. Trends Endocrinol Metab 2013;24:578–587

27. Keuper M, Wernstedt Asterholm I, Scherer PE, et al. TRAIL (TNF-related apoptosis-inducing ligand) regulates adipocyte metabolism by caspase-mediated cleavage of PPARgamma. Cell Death Dis 2013;4:e474

28. Zoller V, Funcke JB, Keuper M, et al. TRAIL (TNF-related apoptosis-inducing ligand) inhibits human adipocyte differentiation via caspase-mediated down-regulation of adipogenic transcription factors. Cell Death Dis 2016;7:e2412
29. Pahar B, Lackner AA, Veazey RS. Intestinal double-positive CD4+CD8+ T cells are highly activated memory cells with an increased capacity to produce cytokines. Eur J Immunol 2006;36:583–592
30. Lumeng CN, Bodzin JL, Saltiel AR. Obesity induces a phenotypic switch in adipose tissue macrophage polarization. J Clin Invest 2007;117:175–184
31. Hotamisligil GS, Shargill NS, Spiegelman BM. Adipose expression of tumor necrosis factor-alpha: direct role in obesity-linked insulin resistance. Science 1993;259:87–91
32. Wueest S, Rapold RA, Schumann DM, et al. Deletion of Fas in adipocytes relieves adipose tissue inflammation and hepatic manifestations of obesity in mice. J Clin Invest 2010;120:191–202
33. Blüher M, Klöting N, Wueest S, et al. Fas and FasL expression in human adipose tissue is related to obesity, insulin resistance, and type 2 diabetes. J Clin Endocrinol Metab 2014;99:E36–E44
34. Funcke JB, Zoller V, El Hay MA, Debatin KM, Wabitsch M, Fischer-Posovszky P. TNF-related apoptosis-inducing ligand promotes human preadipocyte proliferation via ERK1/2 activation. FASEB J 2015;29:3065–3075
35. Gao J, Wang D, Liu D, et al. Tumor necrosis factor-related apoptosis-inducing ligand induces the expression of proinflammatory cytokines in macrophages and re-educates tumor-associated macrophages to an antitumor phenotype. Mol Biol Cell 2015;26:3178–3189
36. Yao Z, Zhang P, Guo H, et al. RIP1 modulates death receptor mediated apoptosis and autophagy in macrophages. Mol Oncol 2015;9:806–817
37. Maixner N, Bechor S, Vershinin Z, et al. Transcriptional dysregulation of adipose tissue autophagy in obesity. Physiology (Bethesda) 2016;31:270–282
38. Bernardi S, Zauli G, Tikellis C, et al. TNF-related apoptosis-inducing ligand significantly attenuates metabolic abnormalities in high-fat-fed mice reducing adiposity and systemic inflammation. Clin Sci (Lond) 2012;123:547–555
39. Forde H, Harper E, Davenport C, et al. The beneficial pleiotropic effects of tumour necrosis factor-related apoptosis-inducing ligand (TRAIL) within the vasculature: a review of the evidence. Atherosclerosis 2016;247:87–96
40. von Karstedt S, Montinaro A, Walczak H. Exploring the TRAILs less travelled: TRAIL in cancer biology and therapy. Nat Rev Cancer 2017;17:352–366
41. Tougaard P, Martinsen LO, Lützhøft DO, et al. TL1A regulates adipose-resident innate lymphoid immune responses and enables diet-induced obesity in mice. Int J Obes 2020;44:1062–1074
42. Wu C, Chen X, Shu J, Lee CT. Whole-genome expression analyses of type 2 diabetes in human skin reveal altered immune function and burden of infection. Oncotarget 2017;8:34601–34609
43. Richard AC, Ferdinand JR, Meylan F, Hayes ET, Gabay O, Siegel RM. The TNF-family cytokine TL1A: from lymphocyte costimulator to disease co-conspirator. J Leukoc Biol 2015;98:333–345
44. Migone TS, Zhang J, Luo X, et al. TL1A is a TNF-like ligand for DR3 and TR6/DcR3 and functions as a T cell costimulator. Immunity 2002;16:479–492
45. Taraban VY, Slebioda TJ, Willoughby JE, et al. Sustained TL1A expression modulates effector and regulatory T-cell responses and drives intestinal goblet cell hyperplasia. Mucosal Immunol 2011;4:186–196
46. Bamias G, Siakavellas SI, Stamatelopoulos KS, Chryssochoou E, Papamichael C, Sfikakis PP. Circulating levels of TNF-like cytokine 1A (TL1A) and its decoy receptor 3 (DcR3) in rheumatoid arthritis. Clin Immunol 2008;129:249–255
47. Konsta M, Bamias G, Tektonidou MG, Christopoulos P, Iliopoulos A, Sfikakis PP. Increased levels of soluble TNF-like cytokine 1A in ankylosing spondylitis. Rheumatology (Oxford) 2013;52:448–451
48. Fang L, Adkins B, Deyev V, Podack ER. Essential role of TNF receptor superfamily 25 (TNFRSF25) in the development of allergic lung inflammation. J Exp Med 2008;205:1037–1048